Applied and Environmental Microbiology, Mar. 2009, p. 1445–1449 Vol. 75, No. 5
0099-2240/09/$08.00+0 doi:10.1128/AEM.02039-08

Simultaneous Interferometric Measurement of Corrosive or Demineralizing Bacteria and Their Mineral Interfaces▽†

M. S. Waters,[1] M. Y. El-Naggar,[2] L. Hsu,[3] C. A. Sturm,[4] A. Luttge,[4] F. E. Udwadia,[5] D. G. Cvitkovitch,[6] S. D. Goodman,[7] and K. H. Nealson[2]*

University of Southern California, Department of Molecular and Computational Biology, 1050 Childs Way MCB 201B, Los Angeles, California 90089-2910[1]; University of Southern California, Department of Geobiology, 835 W. 37th St. SHS 562, Los Angeles, California 90089[2]; University of Southern California, Department of Environmental Engineering, 835 W. 37th St. SHS 562, Los Angeles, California 90089[3]; Rice University, Department of Earth Science, MS-126, 6100 S. Main St., Houston, Texas 77005[4]; University of Southern California, Department of Aerospace and Mechanical Engineering, Viterbi School of Engineering, OHE 430K, Los Angeles, California 90089-1453[5]; University of Toronto, Faculty of Dentistry, Department of Oral Microbiology, 124 Edward St., Rm. 449A, Toronto, Ontario, Canada M5G 1G6[6]; and University of Southern California, Norris School of Dentistry, Division of Diagnostic Sciences, 925 W. 34th St. DEN 4108, Los Angeles, California 90089-0641[7]

Received 2 September 2008/Accepted 26 December 2008

Here, we report simultaneous surface profile measurements of several bacterial species involved in microbially influenced corrosion and their solid-surface interfaces by using vertical scanning interferometry. The capacity to nondestructively quantify microscale topographic changes beneath a single bacterium without its removal offers a unique opportunity to examine in vivo microbe-surface interactions.

As microbiology advances, the relevance of bacterial surface interaction has become abundantly apparent, and the study of microbial communities attached to surfaces (also known as biofilms) has become a major focus. As biofilms form and develop, the surfaces to which they selectively attach may be altered through the activities of the resident microbes, as in microbially influenced corrosion, involving the release of chemicals or the deposition of electrochemically active minerals that accelerate surface demineralization and corrosion, with repercussions spanning from cavity formation in teeth to pit development on a ship's hull (1–4, 6–8, 10, 11, 15, 17–20). Current methods for the characterization of altered surfaces require the removal of the causative bacteria, terminating the process. Noninvasive, visual methods that provide a quantitative understanding of a corroding solid surface and associated bacterial interactions are highly desirable.

Here, we describe the use of vertical scanning interferometry (VSI) to directly measure the surface profiles of both microbes and the surface beneath them. VSI, a rapid, noncontact, minimally invasive technology, combines reflected-light microscopy with Mirau interference optics, using the wave properties of light to precisely define a vertical dimension, with resolutions of <1 μm laterally and <1 nm vertically (12–14). Light reflected from the sample (returned as interferometric fringes) is converted into graphical data called a correlogram and analyzed for peaks to extrapolate the height (z dimension) for every pixel of an image, resulting in a topographical map of a surface (see Fig. S1 and S2 in the supplemental material).

Previously, we described bacterial imaging artifacts associated with light reflected from the surface beneath the bacteria (21). Expanding on techniques used to measure thin-film depth (16), we hypothesized that making minor changes in data acquisition and interpretation would allow us to use the light reflected from both the bacteria and their interface to (i) correct VSI imaging artifacts commonly seen when attempting to visualize bacteria on a surface and (ii) access a second set of fringes from the surface beneath a bacterium.

To evaluate imaging defects on a larger scale, the evaporating edges of several different water drops on mirror steel were scanned by VSI (Fig. 1). Correlogram analyses of a series of points along each drop, moving from deep to shallow, revealed five factors key to imaging interfaces though transparent particles: (i) two correlogram peaks were acquired for every pixel of the video where water covered the polished steel, versus one correlogram peak per pixel for dry polished steel; (ii) as the water depth decreased, so did the distance between the two peaks; (iii) if the amplitude of peak 1 was greater than that of peak 2, then the expected three-dimensional (3-D) image height was obtained, and if the amplitude of peak 1 was less than that of peak 2, then the 3-D image height was lower than expected; (iv) based on a known location of the steel, by using the first peak, the actual height of the water's surface was calculated; and (v) the second peak corresponded to the known location of the steel after correction for the known refractive index (see the supplemental material).

In this approach, when a correlogram for a bacterium is acquired, the peak amplitude defines the surface reflectivity and the distance between peaks defines the thickness (the distance from the microbe surface to the interface) after correction for refractive index changes (see Fig. S3 in the supple-

* Corresponding author. Mailing address: University of Southern California, Department of Geobiology, 835 W. 37th St. SHS 562, Los Angeles, CA 90089. Phone: (213) 821-2511. Fax: (213) 740-8801. E-mail: knealson@usc.edu.

† Supplemental material for this article may be found at http://aem.asm.org/.

▽ Published ahead of print on 5 January 2009.

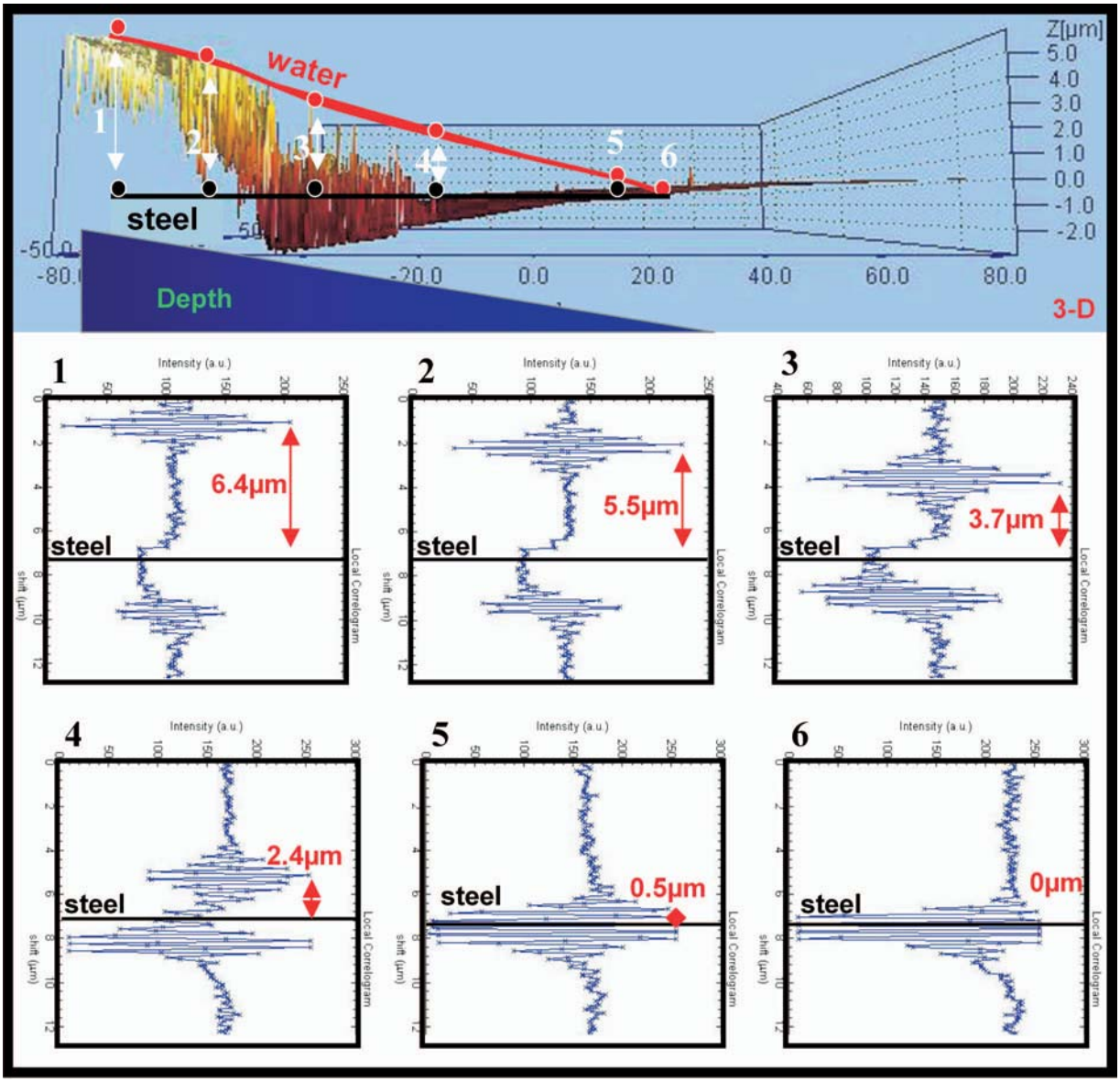

FIG. 1. Measurement of the edge of a drop of water and its steel interface. Above the correlograms is a 3-D height map of the edge of a drop of water on polished steel, made using current software. Current software, clearly, has miscalculated the locations of points 3 to 5. Superimposed is a recalculation of the height of the water surface at all six points (displayed as red dots and a red line), based on the interpretation of the correlograms below. The black dots with the black line are the calculation of the location of the underlying steel surface after correction for the refractive index. Below are correlograms for the six points throughout the drop of water, moving from deep to shallow. These correlograms were used to calculate the depth of the water at each of the six points and the location of the steel. The black line in each correlogram represents the height of the steel after correction for the index of refraction. The measurements in red indicate the distance of the first peak from the steel surface, corresponding to the depth of the water at each of the six points. a.u., arbitrary units.

mental material). Using facultative anaerobe *Shewanella oneidensis* MR-1, a metal oxide-reducing bacterium capable of protecting steel from corrosion (5), we measured bacterial height on polished mirror steel. Height measurements were highly variable; individual bacteria with no morphological abnormalities (as determined by environmental scanning electron microscopy) were commonly interpreted as structures that sat both above and below the steel surface (Fig. 2A), and two-peak correlograms from each area supported the amplitude and height findings from the water experiments described above (Fig. 2B). Measurements made via scanning near-field optical microscopy, a method that measures light passage through a medium, confirmed translucence variability within a single cell, consistent with VSI height measurement variability (data not shown).

To expand the range of VSI data acquisition to conditions that were suboptimal in reflectivity but were known to be capable of corroding or demineralizing a particular substrate, we measured *S. oneidensis* MR-1 on calcite (Fig. 3A), *Streptococcus mutans* UA159 on hydroxyapatite (Fig. 3B),

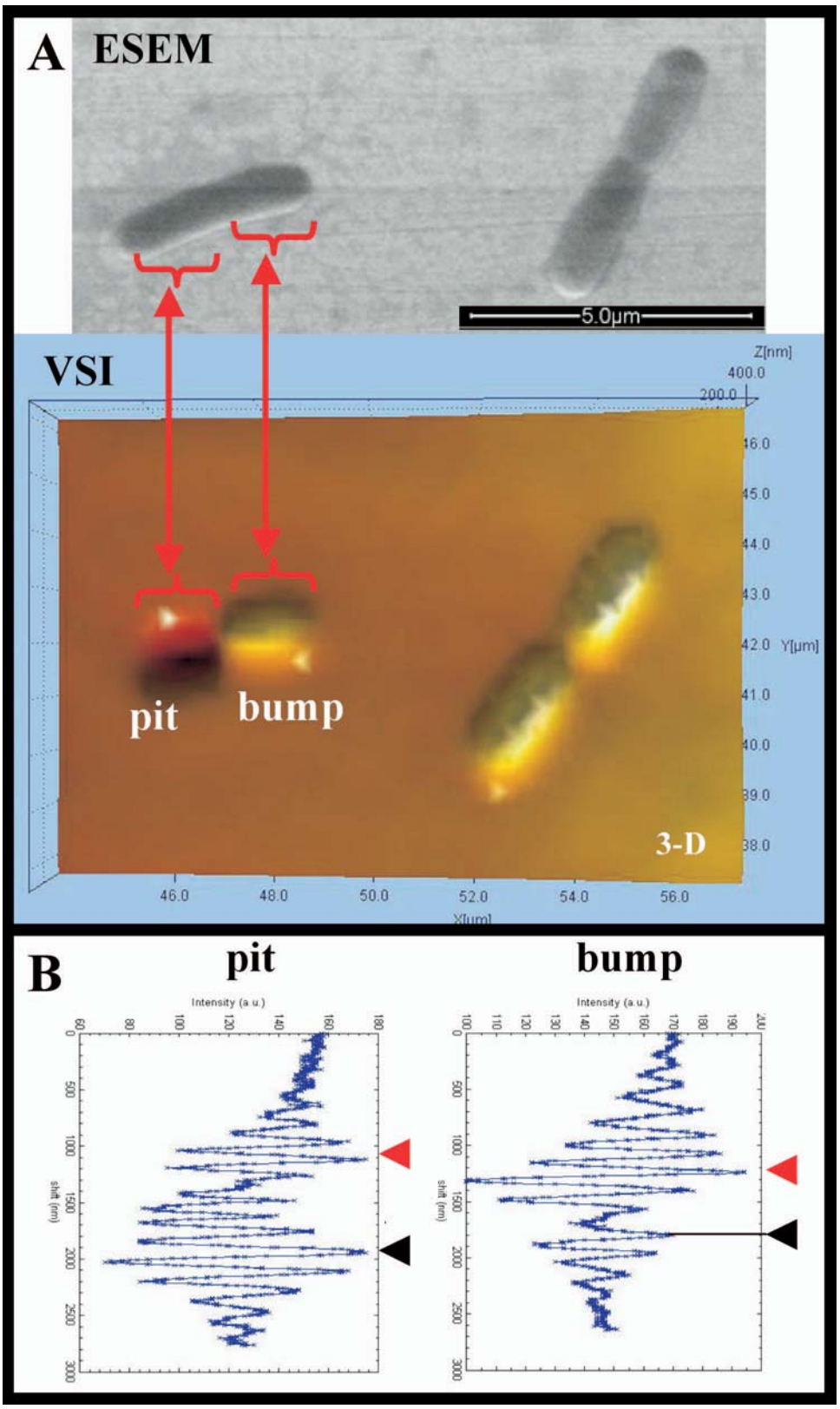

FIG. 2. Comparison of VSI images of *S. oneidensis* MR-1 on steel that measure above and below a polished steel surface. (A) Comparison of images of a single MR-1 bacterium that measures both as a pit in the steel and as a bump on the steel by VSI (bottom panel) and measures normally under an environmental scanning electron microscope (ESEM) (top panel). (B) Comparison of correlograms for a bacterium that falsely measures as a pit and a bacterium that measures normally (as a bump). If the amplitude of peak 1 (red arrowheads) is smaller than that of peak 2 (black arrowheads), then the bacterium appears as a pit (left panel). If the amplitude of peak 1 is larger than that of peak 2, then the bacterium appears as a bump on the surface of the steel (right panel). In both the environmental scanning electron microscope and VSI images, two additional bacteria that appear normally are displayed to the left for comparison. a.u., arbitrary units.

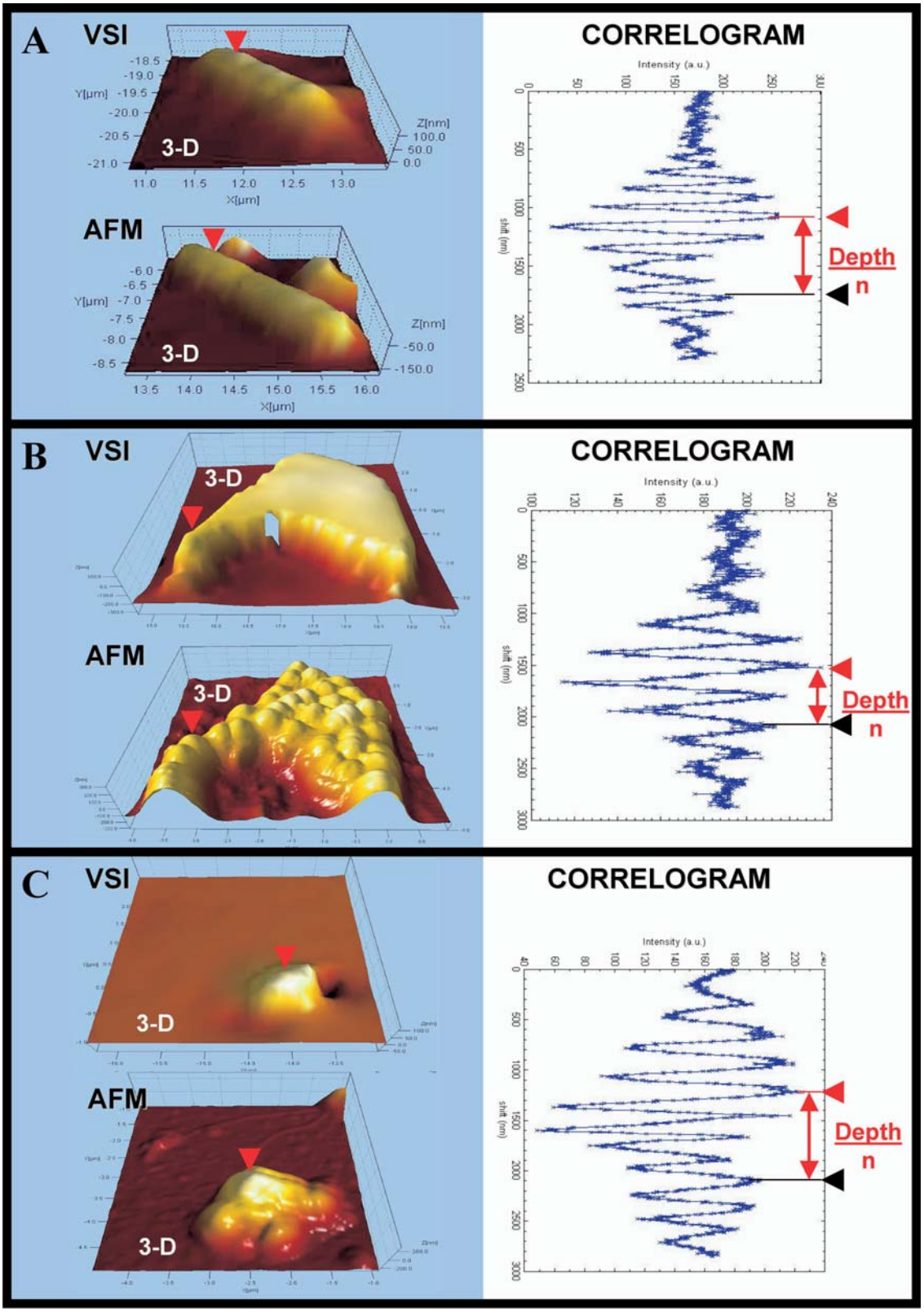

FIG. 3. Measurement of demineralizing or corrosive bacteria and their interface with a biologically relevant substrate. For all image sections, the left panels show overlapping 3-D measurements of bacteria made by VSI (top) and an atomic force microscope (AFM; bottom). The red arrowheads in both images mark the pixel where the correlogram (right) was acquired from a VSI scan. The red arrowheads to the right of the correlograms highlight the peak indicative of the bacterial surface. The black arrowheads highlight the peak indicative of the interface. (A) *S. oneidensis* MR-1 on calcite. The black arrowhead highlights the peak indicative of the calcite surface. (B) *S. mutans* UA159 on hydroxyapatite. The black arrowhead highlights the peak indicative of the hydroxyapatite surface. (C) Sulfate-reducing bacteria on steel. The black arrowhead highlights the peak indicative of the steel surface. a.u., arbitrary units.

and a sulfate-reducing bacterium isolated from environmental sludge on steel (Fig. 3C); each of these organisms is known to be involved in the corrosion or demineralization of the respective contacting substrate. VSI measurements of the bacteria (confirmed to be accurate by atomic force microscopy) consistently resulted in two correlogram peaks. Current VSI software can improperly calculate the pixel height of a transparent particle on a surface, resulting in height measurement errors, such as the false pit in the VSI image in Fig. 3C. Each calculated bacterial height, based on the first correlogram peak, yielded an expected measurement, regardless of 3-D height map defects generated with current VSI software (Fig. 3; data not shown).

In this study, we have shown how to (i) correct imaging artifacts generated with current software and (ii) simultaneously measure a bacterial surface and the surface on which it sits, without removing the potentially active surface-modifying bacteria. This constitutes the first step toward our goal of directly measuring surface modifications (dissolution or deposition) as they occur. With the adaptation of VSI for higher resolution, minor software adjustments, and calibration improvements, we should be able not only to measure dissolution beneath a single cell in real time but also to pinpoint the location where microbially influenced corrosion actually begins (if any exists). For more detail on making accurate measurements, see the supplemental material.

Clearly, the ability to noninvasively study the microbe or particle-solid interface in real time has broad relevance, ranging from microbial ecology to medicine to material sciences and semiconductors. By understanding the nature of microbe-solid interface interactions, it may be possible to have an impact on processes such as microbially influenced corrosion, caused by sulfate-reducing bacteria that electrochemically corrode steel, or medical processes, such as the demineralization of tooth enamel by *S. mutans* lactic acid secretions (6, 9, 20). By directly visualizing real-time height changes in the microbe-mineral interface and refractive index changes to a bacterial population using modifications proposed in this study, we should be able to gain insight into the processes by which bacterial biofilms modify their interactive surfaces.

This work was supported by Office of Naval Research award no. N00014-06-1-0115 and MURI award no. FA9550-06-1-0292 to K.H.N. and by a grant from the AFOSR (DoD).

We thank the USC NanoBiophysics Core Facility for the use of the atomic force microscope.

REFERENCES

1. **Characklis, W. G.** 1990. Int. Workshop Ind. Biofouling Biocorrosion, 13 to 14 September 1990, abstr. 90–004.
2. **Characklis, W. G., W. Lee, B. Peyton, and Z. Lewandowski.** 1990. Interactions between process waters, microbial biofilms, and metal substrata, p. 2/59–2/63. *In* N. J. Dowling, M. W. Mittelman, and J. C. Danko (ed.), Microbial influenced corrosion and biodeterioration. International Congress on Microbially Induced Corrosion, Knoxville, TN, October 1990. The University of Tennessee, Knoxville, TN.
3. **Costerton, J. W., and J. Boivin.** 1990. The role of biofilms in microbial corrosion, p. 5/85–5/89. *In* N. J. Dowling, M. W. Mittelman, and J. C. Danko (ed.), Microbial influenced corrosion and biodeterioration. International Congress on Microbially Induced Corrosion, Knoxville, TN, October 1990. The University of Tennessee, Knoxville, TN.
4. **Cunliffe, D., C. A. Smart, C. Alexander, and E. N. Vulfson.** 1999. Bacterial adhesion at synthetic surfaces. Appl. Environ. Microbiol. **65:**4995–5002.
5. **Dubiel, M., C. H. Hsu, C. C. Chien, F. Mansfeld, and D. K. Newman.** 2002. Microbial iron respiration can protect steel from corrosion. Appl. Environ. Microbiol. **68:**1440–1445.
6. **Featherstone, J. D. B.** 2000. The science and practice of caries prevention. J. Am. Dent. Assoc. **131:**887–899.
7. **Hamilton, W. A.** 2000. Microbially influenced corrosion in the context of metal microbe interactions, p. 419–434. *In* L. V. Evans (ed.), Biofilms: recent advances in their study and control. Harwood Academic Publishers, Amsterdam, The Netherlands.
8. **Jefferson, K.** 2004. What drives bacteria to produce a biofilm? FEMS Microbiol. Lett. **236:**163–173.
9. **Koch, G. H., M. P. H. Brongers, N. G. Thompson, Y. P. Virmani, and J. H. Payer.** 2002. Corrosion costs and preventive strategies in the United States. NACE International, Houston, TX.
10. **Lewandowski, Z., W. Dickinson, and W. Lee.** 1997. Electrochemical interactions of biofilms with metal surfaces. Water Sci. Technol. **36:**295.
11. **Little, B. J., P. A. Wagner, and Z. Lewandowski.** 1998. The role of biomineralization in microbiologically influenced corrosion, p. 294/1–294/18. *In* Proceedings of the CORROSION/98 Research Topical Symposia. NACE International, Houston, TX.
12. **Luttge, A.** 2004. Crystal dissolution kinetics studied by vertical scanning interferometry (VSI) and Monte Carlo simulations: a brief review and outlook, p. 209–247. *In* X.-Y. Liu and J. De Yoreo (ed.), Nanoscale structure and assembly at solid-fluid interfaces, vol. 1. Kluwer Academic Publishers, Dordrecht, The Netherlands.
13. **Luttge, A.** 2003. Vertical scanning interferometry: super-resolution and *in situ* capabilities for the studies of gashydrates. Energy Explor. Exploitation **21:**329–331.
14. **Luttge, A., E. W. Bolton, and A. C. Lasaga.** 1999. An interferometric study of the dissolution kinetics of anorthite: the role of relative surface area. Am. J. Sci. **299:**652.
15. **Shi, X., R. Avci, and Z. Lewandowski.** 2002. Microbially deposited manganese and iron oxides on passive metals—their chemistry and consequences for material performance. Corrosion **58:**728.
16. **Sun, C., L. Yu, Y. Sun, and Q. Yu.** 2005. Scanning white-light interferometer for measurement of the thickness of a transparent oil film on water. Appl. Opt. **44:**5202.
17. **Svensater, G., J. Welin, J. C. Wilkins, D. Beighton, and I. R. Hamilton.** 2001. Protein expression by planktonic and biofilm cells of *Streptococcus mutans*. FEMS Microbiol. Lett. **205:**139–146.
18. **Toes, G. J., K. W. Van Muiswinkel, W. Van Oeveren, A. J. H. Suurmeijer, W. Timens, I. Stokroos, and J. J. A. M. Van den Dungen.** 2002. Superhydrophobic modification fails to improve the performance of small diameter expanded polytetrafluoroethylene vascular grafts. Biomaterials **23:**255.
19. **Van Loosdrecht, M. C. M., W. Norde, J. Lyklema, and A. J. B. Zehnder.** 1990. Hydrophobic and electrostatic parameters in bacterial adhesion. Aquat. Sci. **52:**1015.
20. **Videla, H. A., and L. K. Herrera.** 2005. Microbiologically influenced corrosion: looking to the future. Int. Microbiol. **8:**169–180.
21. **Waters, M. S., C. A. Sturm, M. Y. El-Naggar, A. Luttge, F. E. Udwadia, D. G. Cvitkovitch, S. D. Goodman, and K. H. Nealson.** 2008. In search of the microbe/mineral interface: quantitative analysis of bacteria on metal surfaces using vertical scanning interferometry. Geobiology **6:**254–262.